ADVANCED ENGINEERING MATERIALS
www.aem-journal.com

Multidipping Technique for Fabrication Time Reduction and Performance Improvement of Solution-Processed Single-Walled Carbon Nanotube Thin-Film Transistors

Hyeonggyu Kim, Jiseok Seo, Narkhyeon Seong, Seunghwan Lee, Sooyeon Lee, Taehoon Kim, and Yongtaek Hong**

Herein, a simple and effective technique, "multidipping technique," is implemented to rapidly form random networks of single-walled carbon nanotubes (SWCNTs) used as a channel material in solution-processed thin-film transistors (TFTs). The multidipping process consists of repetition of dipping a substrate into a dispersed semiconducting SWCNT solution and rinsing the substrate between each dipping process. Compared with the conventional dipping method, this technique reduces total deposition time required to form high-quality SWCNT networks by more than half and simultaneously improves the electrical performances of SWCNT TFTs. These phenomena are also comprehensively analyzed with experiments and microscopic images of the channel region, which well show morphology of the SWCNT networks. It is believed that the low-temperature process and facile deposition method of SWCNT networks can provide a guideline for high-throughput fabrication of high-performance SWCNT TFT arrays in flexible active matrix sensor array and display applications.

1. Introduction

Solution-processed thin-film transistor (TFT) has attracted much attention because it is a promising device to meet the demand for various applications, such as wearable devices and displays. Various active materials, for example, organic, oxide, and carbon-based materials, have been investigated.[1–6] Among them, solution-processed random networks of single-walled carbon nanotubes (SWCNTs) have been widely studied due to their high intrinsic carrier mobility, mechanical flexibility, and good transparency.[7–14] Furthermore, highly purified semiconducting SWCNTs with dispersed ink are widely used for large-area flexible electronics, such as logic circuits, active-matrix pixel, and biosensor arrays, because it is possible to fabricate the devices at the low temperatures.[10,14–21] To implement reliable large-area arrays based on SWCNT TFTs, various solution-based deposition techniques of SWCNT networks have been investigated, including direct dipping,[15,18–20] spin-coating,[13,22] gravure printing,[15,23] aerosol jet printing,[24,25] and inkjet printing.[26,27] Direct patterning technology such as gravure and inkjet printing has advantages of economical material usage and no additional patterning process such as photolithography and oxygen plasma etching. However, many research groups have used the dipping method because it features high uniformity over large area, low process complexity, and low degree of contamination compared with other deposition methods.[28,29]

However, when the SWCNT TFTs are manufactured by the dipping method, throughput is generally low due to a very long deposition time of SWCNT, especially with aqueous SWCNT solution.[15,16,20,28,29] It is noted that various surfactant materials, such as sodium dodecyl sulfate (SDS), sodium dodecylbenzene sulfonate (SDBS), and sodium cholate (SC), are used to form well-dispersed aqueous SWCNT solution with long-term dispersion stability. Among them, alkyl-chain-based surfactants, widely used for effective additives, generally counteract against SWCNT film formation and repulsive force caused by them makes deposition time much longer like a few hours to even a week.[28,29] The more stable the ink is, the longer the deposition time is. One way to reduce the deposition time of SWCNT is using SWCNT ink based on organic solvent such as 1-methyl-2-pyrrolidone (NMP) because the surfactant is not necessary while dispersing the SWCNT in organic solvents. However, it is not suitable for some polymeric substrates and dielectrics due to chemical attack by the used solvents, so that there is a limitation for flexible or stretchable electronics.[30–32] In our previous research, we significantly reduced the total deposition time of SWCNTs by adding certain amounts of diluted acid into the commercial aqueous SWCNT ink. Because acid decreases pH of the solution and modifies the zeta potential of the solution, it reduces the repulsive force of the surfactant. The deposition time, therefore, is significantly reduced compared with as-purchased aqueous SWCNT ink. In contrast, as the pH of the solution is lowered, the dispersion stability of the ink could be degraded because the ionic surfactants attached at SWCNT are modified.[19]

H. Kim, J. Seo, N. Seong, S. Lee, Prof. S. Lee, Dr. T. Kim, Prof. Y. Hong
Department of Electrical and Computer Engineering
Inter University Semiconductor Research Center (ISRC)
Seoul National University
Seoul 08826, Republic of Korea
E-mail: rhlight4@snu.ac.kr; yongtaek@snu.ac.kr

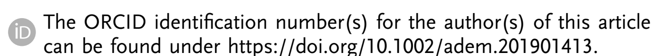
The ORCID identification number(s) for the author(s) of this article can be found under https://doi.org/10.1002/adem.201901413.

DOI: 10.1002/adem.201901413

 © 2020 WILEY-VCH Verlag GmbH & Co. KGaA, Weinheim

In this work, we present another simple and effective technique, multidipping technique, to rapidly form a dense SWCNT film at the channel region with a short deposition time. As mentioned before, many research groups have so far used the "one-time dipping" method where the substrate is dipped only once in SWCNT ink with a very long time.[14,16,20] Rather, by applying "multidipping" method where the substrate is repeatedly dipped in SWCNT inks for a very short time during each dipping process and rinsed between the multiple dipping steps, we significantly reduced the total deposition time and improved TFT performances at the same time. It is noted that in our newly proposed technique, the as-purchased SWCNT ink is used and thus, the dispersion stability of the original solution does not degrade.

2. Experimental Section

2.1. Fabrication of SWCNT TFT with Multidipping Technique

Figure 1a shows the overall fabrication process of SWCNT TFTs with the multidipping technique. First, heavily doped p-type Si with thermally grown SiO_2 wafer was cleaned with acetone and then isopropyl alcohol (IPA) for 20 min in ultrasonic bath for each solvent, blown with nitrogen (N_2) gun, and baked in oven at 100 °C for 40 min. Then, the wafer was exposed with ultraviolet ozone (UVO) lamp in chamber for 10 min to form hydroxyl group on its surface. After that, poly-L-lysine (PLL) solution (aqueous solution, 0.1% (w/v) in H_2O, Sigma-Aldrich Corp.) was drop-casted for 10 min on the UVO-treated substrate, and it was rinsed with deionized (DI) water for 1 min and blown with N_2 gun sequentially to form the amine-functionalized surface on the wafer. Although amine-functionalized substrate was dipped into as-purchased 95% semiconducting-enriched SWCNT ink (IsoNanotube-S, Nanointegris Corp.) for a very long time, rinsed with DI water for 1 min, and blown with N_2-gun in one-time dipping method, in multidipping method, the substrate was dipped into SWCNT ink for 1 min, rinsed, and blown with the same recipe, and this procedure was repeated many times to form a high-quality networks in the channel area. SWCNT density in the channel area depends on the number of iteration in the multidipping method, whereas it depends on the deposition time in the one-time dipping method (**Figure 2**). On the SWCNT layer, source and drain electrodes were inkjet-printed with piezoelectric-type inkjet-printer (DMP-2831, Dimatix Corp.) using metal–organic-based silver ink (JET-004T, Kunshan Hisense Electronic Corp.). TFTs with the bottom gate and top contact structure were formed, as shown in Figure 1b. Figure 1c shows the optical image of the channel region with the inkjet-printed source/drain Ag electrodes. Length (L) and width (W) of the channel are 160 and 180 μm, respectively. More than ten devices were fabricated on a $2 \times 2\,cm^2$ silicon wafer and the SWCNT layer of each device was physically isolated using a hard tip to remove unnecessary current path.

2.2. Measurement

Electrical properties of the SWCNT TFTs such as transfer and output characteristics were measured with agilent 4155C semiconducting parameter analyzer. Also, the optical images of channel region were obtained with optical microscope (DSX510, Olympus Corp.). Morphology of channel regions was analyzed with AFM equipment (XE-100, Parks' System Corp.).

3. Results and Discussion

Figure S1, Supporting Information, shows the measured results of the fabricated TFTs and Figure 2 shows the transfer characteristic of representative data of each case, which has very similar on-current level between one-time dipping and multidipping. For as-purchased SWCNT inks, significantly long deposition times were required to observe a reasonable TFT performance

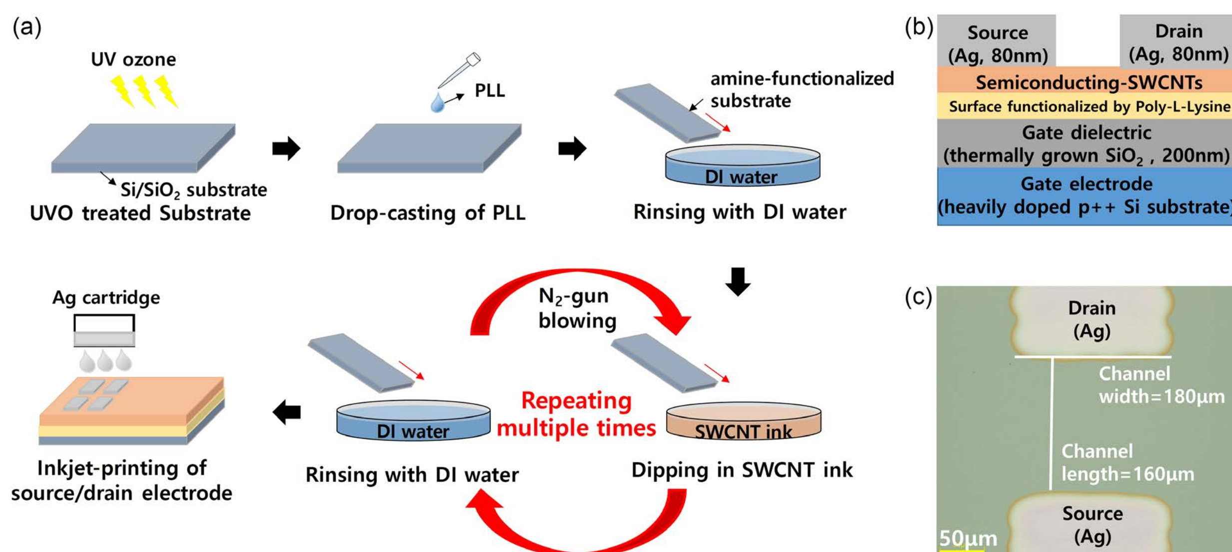

Figure 1. a) Fabrication process of SWCNT TFTs with multidipping technique. b) Schematic of SWCNT TFT structure. c) Optical image of device channel region with inkjet-printed source and drain Ag electrodes.

© 2020 WILEY-VCH Verlag GmbH & Co. KGaA, Weinheim

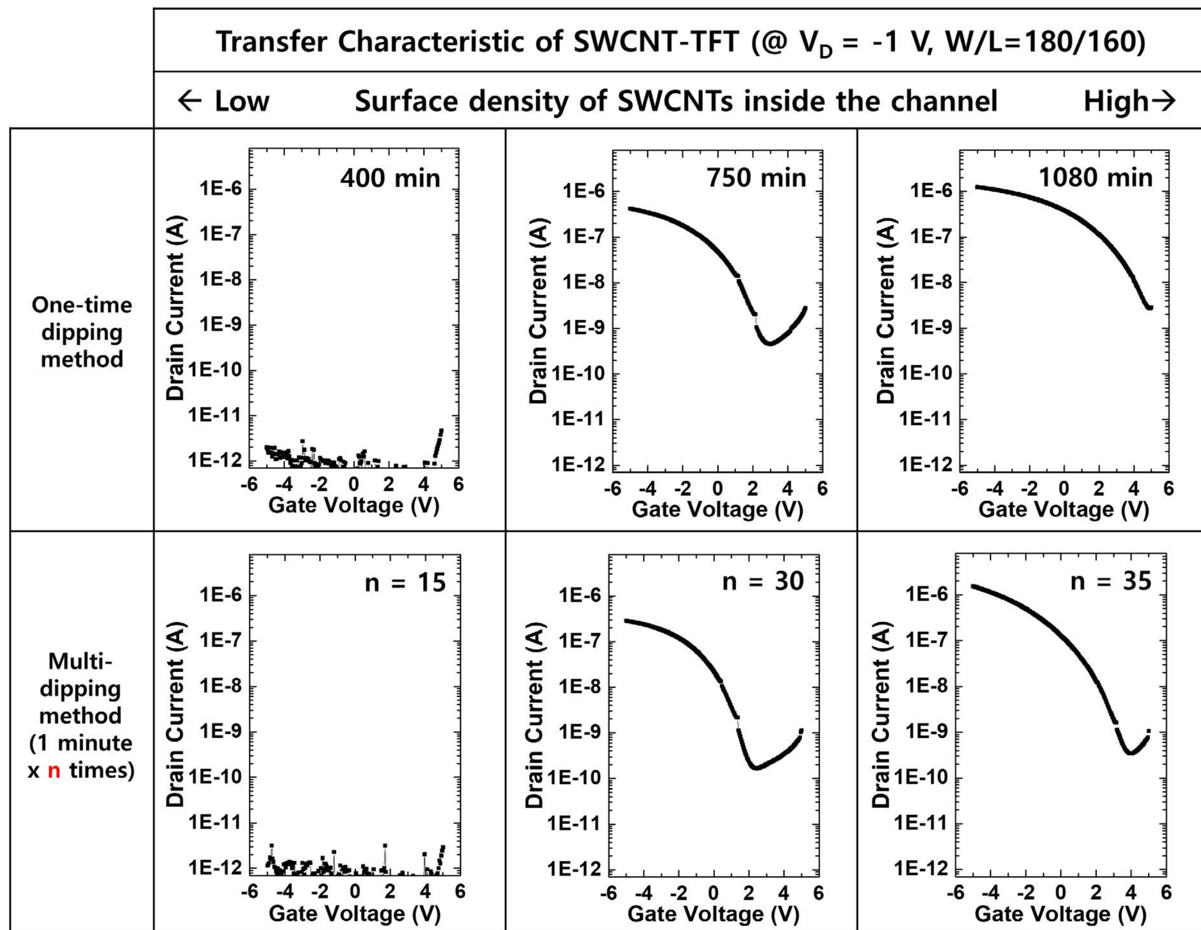

Figure 2. Transfer characteristics of one-time dipping and multidipping devices which have almost same on-current level, which depends on the densities of SWCNT networks. The densities were controlled by dipping time and number of dipping iteration for each case, respectively (representative data from Figure S1, Supporting Information).

in the one-time dipping method. It is noted that the as-purchased ink has a large amount of surfactant for longer dispersion stability, and thus it takes unexpectedly long to obtain dense SWCNT network in the channel area. In contrast, short deposition time (for example, 750 min vs 1 min × 30 times, and 1080 min vs 1 min × 35 times) was needed to achieve similar on-current levels. Especially in case of 35 times of multidipping, it took about 82 min to totally fabricate the active layer while considering the time of dipping (1 min), rinsing (1 min), and N_2 blowing with handling (20 s) in each step. The 35-time multidipping process, however, still exhibited over 90% time reduction compared with the case of 1080 min of one-time dipping. Therefore, our results clearly show that even though we consider the repetition of 1 min dipping and rinsing steps, the multidipping process significantly reduced the total time for device fabrication.

Table 1 shows the device performances for the case of a high density of SWCNTs in Figure S1, Supporting Information, and Figure 2 (1080 min vs 1 min × 35 times). Field-effect mobility (μ), subthreshold swing (S.S.), and turn-on voltage ($V_{\text{turn-on}}$) are extracted from the transfer characteristics measured at forward sweep (from positive to negative) of gate bias, and we used a conventional field-effect mobility extraction method (Figure S2, Supporting Information).[27,33] For as-purchased inks, when the devices were fabricated with the multidipping method, mobility was increased and turn-on voltage and subthreshold swing were decreased in comparison with those made from the one-time dipping method.

Table 1. Extracted electrical characteristics of devices.

Type	Mobility [cm^2 (V s)$^{-1}$]	Turn-on voltage [V]	S.S. [V dec^{-1}]
a) As-purchased, one-time dipping (18 h)	9.02 ± 0.85	4.77 ± 0.22	1.35 ± 0.20
b) As-purchased, multidipping (1 min × 35 times)	20.74 ± 2.41	3.83 ± 0.31	1.06 ± 0.12

Overall, the multidipping method can significantly reduce the total deposition time of SWCNT and enhance the electrical performances of the devices at as-purchased SWCNT ink, as shown in **Figure 3**a. It is noted that SWCNT deposition is closely related to the electrostatic interaction between the amine-terminated surface and SWCNTs.[32] Due to the residue of the ionic surfactant attached to the amine-terminated substrate and preformed

© 2020 WILEY-VCH Verlag GmbH & Co. KGaA, Weinheim

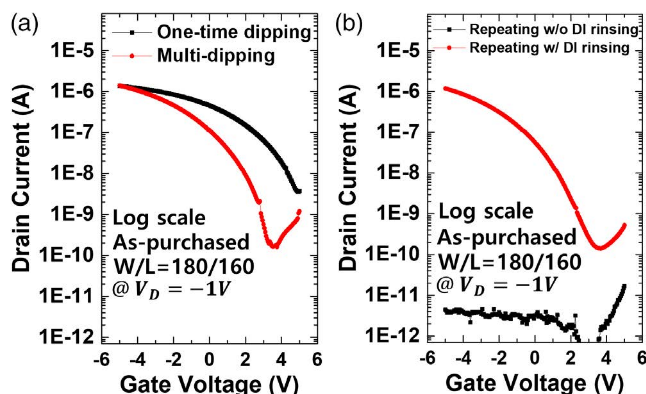

Figure 3. Transfer characteristics of a) devices which have almost same on-current level between one-time dipping and multidipping devices fabricated with as-purchased SWCNT ink (1080 min; 35 times) and b) devices which were fabricated with multidipping technique with and without DI water rinsing.

SWCNT layer, which is mixed in commercialized SWCNT ink to promote its dispersion stability, the repulsive force between the residue and SWCNTs can counteract to the further deposition of the SWCNTs during the dipping process. Therefore, not only does the deposition time of SWCNT get longer with the amount of surfactant in the ink, but also bundled SWCNT network is formed on the substrate because the additional SWCNTs cannot be easily attached on the surfactant-deposited surface where SWCNTs were not preformed.[19,32,34,35] Schematic picture of the situation is shown in Figure S3, Supporting Information. However, by doing multidipping process where rinsing was performed after each dipping process, the total deposition time was significantly reduced for the as-purchased ink because it is well known that rinsing processes with various solvents, such as DI water, IPA, and acetone, remove residue surfactant and weakly attached SWCNTs on the substrate.[18,36–39] We used multiple DI water rinsing between each dipping step of SWCNT, which suppressed counteraction of the residue surfactant at the predeposited SWCNT film and amine-terminated substrate. Consequently, we could not only form the dense and uniform SWCNT network on the substrate but also decrease the total deposition time of SWCNT using the multidipping technique.

To further investigate the effect of rinsing after each dipping step of the multidipping process, we fabricated two types of devices, each of which is from the multidipping process with or without DI water rinsing at each dipping step. In the case of the device without DI water rinsing at each dipping step, DI water rinsing was performed only after the last dipping step. The other procedures of TFT fabrication and the number of iteration were the same in both cases. Figure 3b shows the transfer characteristics of the two types of devices. Devices from the multidipping process without DI water rinsing did not show any TFT characteristics, whereas the ones from the multidipping process with DI water rinsing showed a TFT behavior. It means that the SWCNT network dense enough for a proper TFT performance was formed at channel area for the latter ones but not for the former ones. It is known that devices with proper density of SWCNT (just above the percolation threshold) could exhibit the proper transistor characteristic. As the density of SWCNT increases, on/off current ratio is decreased, due to the increase in the percolation paths through large amount of the tube–tube junction. If the SWCNT films starts to be thicker or much denser than aforementioned percolation threshold, the on/off characteristics of the SWCNT TFTs will be degraded.[21,40–44] In multidipping without DI water rinsing process, even though the SWCNT film is exposed to the air between each dipping step, the deposition mechanism of SWCNT is the same with the one-time dipping. Because there is no rinsing process between each dipping step, the residue also remains and it hinders the additional attachment of SWCNT. Moreover, in the conventional one-time dipping process, the deposition time of SWCNT is as much as 1080 min, whereas multidipping without DI water rinsing takes only 35 min (1 min $\times$ 35 times). So an insufficient SWCNT network is formed in the case of multidipping without DI water rinsing because the deposition time of SWCNT is extremely short compared with the one-time dipping process. Therefore, from the result of multidipping with and without DI water rinsing, we insist that DI water rinsing is a key process to make the sufficient SWCNT network. The principles of three different dipping methods are shown in **Figure 4**.

It is noted that, in one-time dipping device, longer rinsing time may further remove surfactants resulting in performance improvement. However, we only observed slight improvement when we rinsed the one-time dipping device for 30 min (long-time rinsing), in comparison with the 1 min rinsing device (reference) (Figure S4, Supporting Information). We think that once a dense SWCNT network is formed, it is probably difficult to further remove surfactants in the network even though the rinsing time is increased. The multidipping and rinsing process can more effectively remove the surfactant in the network with much shorter total fabrication time. In addition, it should be also noted that unit-dipping time for the multidipping and rinsing process can be further reduced to achieve reduction in the total fabrication time (considering the time of dipping, rinsing, and blowing with handling). However, we found that there would be an optimum unit-dipping time for given ink conditions. The total fabrication time can become longer again for the unit-dipping time shorter than the optimum time because of frequent iteration, and the performance improvement is negligible. In addition, too short multidipping time is difficult to be consistently repeated at each step during the whole fabrication process. In our case, the optimum unit-dipping time was about 1 min considering the total fabrication time, device performances, and repeatable process handling.

To verify the mechanism of SWCNT network formation, we obtained atomic force microscope (AFM) images of the SWCNT film formed from the one-time dipping, and multidipping with and without DI water rinsing processes as shown in **Figure 5**, and compared the morphology of each case. The density and morphology of the SWCNT network at channel area were analyzed using an AFM because these can efficiently show the morphology of random networks of SWCNTs at the channel area.[45]

In optical images (Figure S5, Supporting Information), several impurities exist on the channel region at both the one-time dipping device and the multidipping one. Excess surfactants in the solution and the bundles of SWCNTs are settled on the substrate

© 2020 WILEY-VCH Verlag GmbH & Co. KGaA, Weinheim

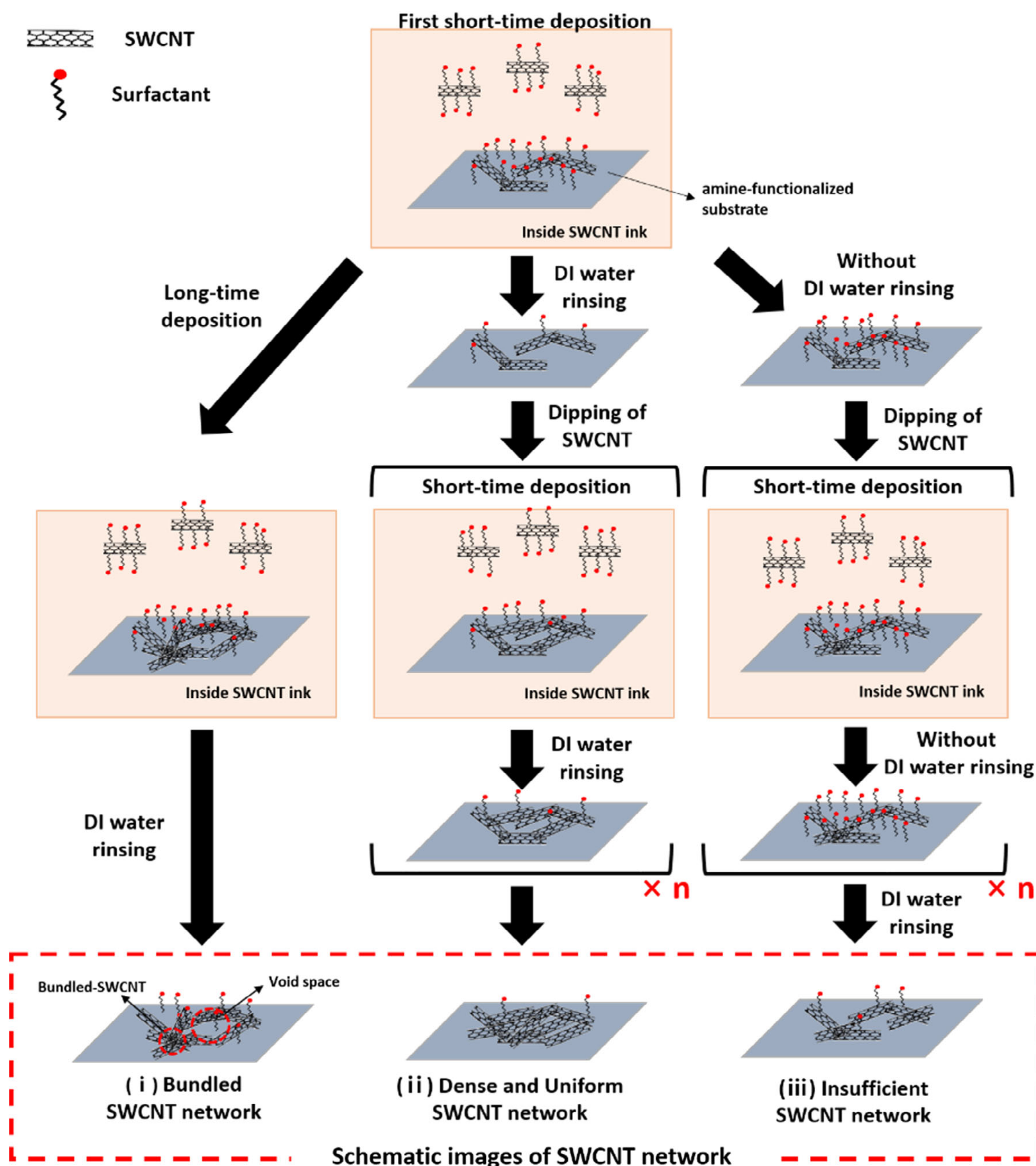

Figure 4. Schematics of principle and fabricated SWCNT network of three different dipping methods, which are one-time dipping, multidipping with DI water rinsing, and multidipping without DI water rinsing.

during the deposition procedure of SWCNTs so that these impurities are formed and degrade the electrical performance of the device.[45] In the multidipping device with DI rinsing between dipping steps, however, more DI water rinsing procedures are performed during fabrication and the deposition time of SWCNTs is short compared with the one-time dipping devices so that the number of impurities of channel region are significantly reduced, resulting in the enhanced electrical performance of multidipping devices. Moreover, there are many void spaces between SWCNTs at the one-time dipping device compared with the multidipping device in AFM images (Figure 5a,b). That means the random networks of SWCNTs are less compact and many bundled SWCNTs are deposited on the substrate at the one-time dipping devices.

In AFM images, we extracted eight lines profiles of the channel area, and checked the RMS values of surface roughness and the peak-to-valley value of each case to obtain the reliability of each value. Among them, the line profiles of the red dotted line in AFM images are shown in Figure 5. Also, we extracted average full width at half maximum (FWHM) value from all peaks in each

© 2020 WILEY-VCH Verlag GmbH & Co. KGaA, Weinheim

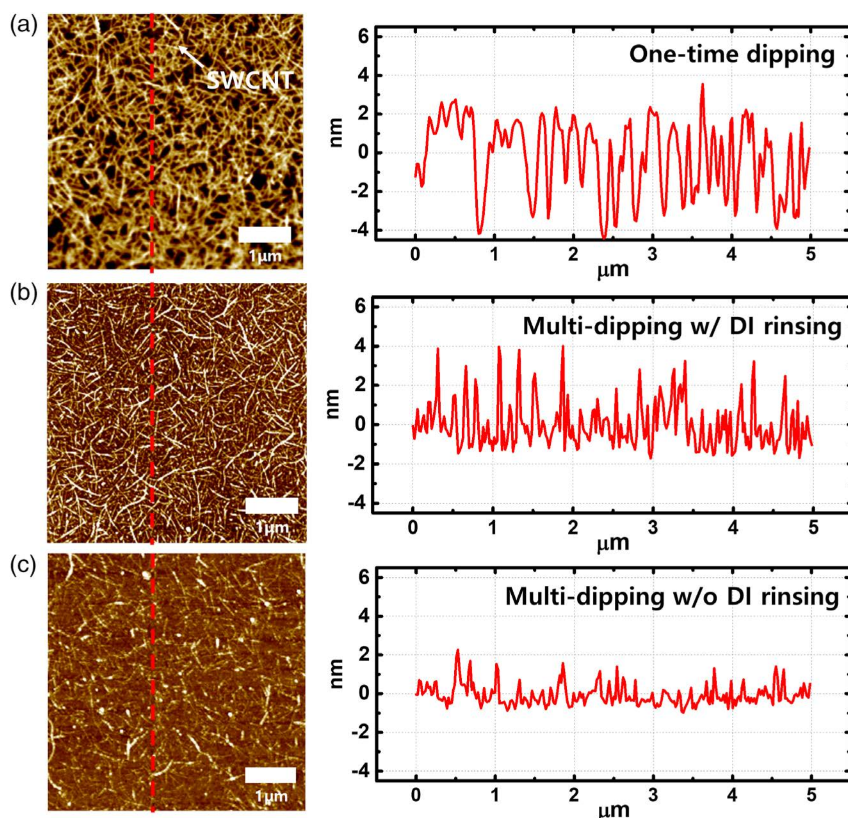

Figure 5. AFM image and line profile extracted from red dotted line in AFM image of the device channel region deposited by a) one-time dipping, b) multidipping with DI water rinsing, and c) multidipping without DI water rinsing device.

line profiles, which is fitted with Gaussian distribution, to analyze the bundle effect inside the SWCNT network effectively. The larger the average value of FWHM is, the more bundled SWCNT network exists at the channel region. All parameters extracted from the line profiles of three cases are shown in **Table 2**.[19,46]

While comparing three parameters between the case of one-time dipping and multidipping with DI water rinsing, all values show much higher in the former one. SWCNTs are more uniformly deposited on the substrate at the multidipping device, whereas many bundles of SWCNTs are formed at the channel network of the one-time dipping device. Generally, these SWCNT bundles at the channel region can degrade the transistors' electrical performance because SWCNTs at the upper side of the bundle can act as charge trap and increase the possibility of transferring the charge between source and drain electrode at off-state so that the device shows more metallic operation. Therefore, the device exhibits high off-current level and turn-off voltage due to the unwanted current path caused by bundled SWCNTs.[45,47,48]

Then, we compared the AFM images and three parameters measured from each line profiles of the multidipping with and without DI water rinsing (Figure 5b,c). When the devices were fabricated with the latter one, less semiconducting SWCNT was deposited and junctions of SWCNTs were not enough to form the current path between the source and drain electrode on the substrate. In contrast, many SWCNTs were densely deposited at the channel region in case of those fabricated with the former one (for example, 52 SWCNTs per 5 μm at the red dotted line in AFM image of Figure 5b vs 17 SWCNTs per 5 μm at the red dotted line in AFM image of Figure 5c.). In Table 2b,c, all values, including the density of SWCNT, are small at multidipping without DI water rinsing device, except for FWHM value. These results also mean, in the multidipping technique, DI water rinsing at each dipping step is a key process to rapidly and densely deposit the SWCNT at the channel region.[18,49,50] Therefore, the device exhibits the proper and excellent TFT characteristics in the multidipping with DI water rinsing.

Table 2. Extracted parameters of three different types of dipping method at line profiles of AFM images.

Types	(a)	(b)	(c)
Parameters	One-time dipping	Multidipping with DI rinsing	Multidipping without DI rinsing
RMS value of surface roughness[a)] [nm]	1.83 ± 0.15	1.24 ± 0.11	0.65 ± 0.06
Peak-to-valley value[b)] [nm]	8.80 ± 1.18	6.72 ± 0.11	3.64 ± 0.34
Average value of FWHM[c)] [nm]	148	38.9	58.5

[a)]Measured data were obtained at eight lines from AFM image; [b)]Measured data were obtained at eight lines from AFM image; [c)]Measured data were obtained from line profiles of Figure 5.

 © 2020 WILEY-VCH Verlag GmbH & Co. KGaA, Weinheim

Overall, our experimental results showed that multidipping devices had significantly reduced deposition time of SWCNT and much better electrical performances in terms of mobility, S.S., and turn-on voltage than that of one-time dipping devices. Based on our optical and AFM images, it can be explained that the random network of SWCNT formed with the multidipping technique is much densely and more uniformly formed compared with that with the one-time dipping technique.

4. Conclusion

In summary, we propose multidipping technique not only for a rapid formation of the random network of semiconducting SWCNTs but also for the high-performance characteristics of SWCNT TFTs. The multidipping process forms the same level of SWCNT network density but in significantly reduced time, by removing repellent surfactant residue and thus enhancing SWCNT deposition, in comparison with the one-time dipping process. We believe that high-performance SWCNT TFTs on various substrates including flexible plastics or stretchable elastomers can be easily fabricated in a very short time with our technique, which can enable early commercialization and mass production of SWCNT TFTs.

Supporting Information

Supporting Information is available from the Wiley Online Library or from the author.

Acknowledgements

This work was financially supported by the R&D Convergence Program of NST (National Research Council of Science and Technology) of Republic of Korea (grant no. CAP-15-04-KITECH).

Conflict of Interest

The authors declare no conflict of interest.

Keywords

multidipping, random networks, semiconducting single-walled carbon nanotubes, solution process, thin-film transistors

Received: November 18, 2019
Revised: February 11, 2020
Published online: February 28, 2020

[1] L. Basiricò, P. Cosseddu, B. Fraboni, A. Bonfiglio, *Thin Solid Films* **2011**, *520*, 1291.
[2] T. Minari, C. Liu, M. Kano, K. Tsukagoshi, *Adv. Mater.* **2012**, *24*, 299.
[3] L. Zhang, W. Xiao, W. Wu, B. Liu, *Appl. Sci.* **2019**, *9*, 773.
[4] J. Jang, R. Kitsomboonloha, S. L. Swisher, E. S. Park, H. Kang, V. Subramanian, *Adv. Mater.* **2013**, *25*, 1042.
[5] C. Yeom, K. Chen, D. Kiriya, Z. Yu, G. Cho, A. Javey, *Adv. Mater.* **2015**, *27*, 1561.
[6] T. Lei, L. L. Shao, Y. Q. Zheng, G. Pitner, G. Fang, C. Zhu, S. Li, R. Beausoleil, H. S. P. Wong, T. C. Huang, K. T. Cheng, Z. Bao, *Nat. Commun.* **2019**, *10*, 2161.
[7] P. Avouris, Z. Chen, V. Perebeinos, *Nat. Nanotechnol.* **2007**, *2*, 605.
[8] K. Kim, B. G. Hyun, J. Jang, E. Cho, Y. G. Park, J. U. Park, *J. Inf. Disp.* **2016**, *17*, 131.
[9] K. Xiao, Y. Liu, P. Hu, G. Yu, X. Wang, D. Zhu, *Appl. Phys. Lett.* **2003**, *83*, 150.
[10] C. Wang, K. Takei, T. Takahashi, A. Javey, *Chem. Soc. Rev.* **2013**, *42*, 2592.
[11] D. M. Sun, M. Y. Timmermans, Y. Tian, A. G. Nasibulin, E. I. Kauppinen, S. Kishimoto, T. Mizutani, Y. Ohno, *Nat. Nanotechnol.* **2011**, *6*, 156.
[12] K. Higuchi, S. Kishimoto, Y. Nakajima, T. Tomura, M. Takesue, K. Hata, E. I. Kauppinen, Y. Ohno, *Appl. Phys. Express* **2013**, *6*, 085101.
[13] M. C. LeMieux, S. Sok, M. E. Roberts, J. P. Opatkiewicz, D. Liu, S. N. Barman, N. Patil, S. Mitra, Z. Bao, *ACS Nano* **2009**, *3*, 4089.
[14] N. Seong, T. Kim, H. Kim, T. J. Ha, Y. Hong, *Curr. Appl. Phys.* **2015**, *15*, S8.
[15] P. H. Lau, K. Takei, C. Wang, Y. Ju, J. Kim, Z. Yu, T. Takahashi, G. Cho, A. Javey, *Nano Lett.* **2013**, *13*, 3864.
[16] D. Lee, J. Yoon, J. Lee, B. H. Lee, M. L. Seol, H. Bae, S. B. Jeon, H. Seong, S. G. Im, S. J. Choi, Y. K. Choi, *Sci. Rep.* **2016**, *6*, 26121.
[17] Y. Deng, M. Zhang, F. Yuan, Z. Li, W. Zhou, *Nano* **2016**, *11*, 1650060.
[18] T. Takahashi, K. Takei, A. G. Gillies, R. S. Fearing, A. Javey, *Nano Lett.* **2011**, *11*, 5408.
[19] T. Kim, N. Seong, J. Ha, H. Kim, T. J. Ha, Y. Hong, *J. Mater. Chem. C* **2016**, *4*, 5461.
[20] L. S. Liyanage, H. Lee, N. Patil, S. Park, S. Mitra, Z. Bao, H. S. P. Wong, *ACS Nano* **2011**, *6*, 451.
[21] C. Wang, J. Zhang, K. Ryu, A. Badmaev, L. G. De Arco, C. Zhou, *Nano Lett.* **2009**, *9*, 4285.
[22] N. Izard, S. Kazaoui, K. Hata, T. Okazaki, T. Saito, S. Iijima, N. Minami, *Appl. Phys. Lett.* **2008**, *92*, 243112.
[23] J. Noh, M. Jung, K. Jung, G. Lee, J. Kim, S. Lim, D. Kim, Y. Choi, Y. Kim, V. Subramanian, G. Cho, *IEEE Electron Device Lett.* **2011**, *32*, 638.
[24] M. Ha, Y. Xia, A. A. Green, W. Zhang, M. J. Renn, C. H. Kim, M. C. Hersam, C. D. Frisbie, *ACS Nano* **2010**, *4*, 4388.
[25] W. Xu, J. Zhao, L. Qian, X. Han, L. Wu, W. Wu, M. Song, L. Zhou, W. Su, C. Wang, S. Nie, Z. Cui, *Nanoscale* **2014**, *6*, 1589.
[26] P. Beecher, P. Servati, A. Rozhin, A. Colli, V. Scardaci, S. Pisana, T. Hasan, A. J. Flewitt, J. Robertson, G. W. Hsieh, F. M. Li, A. Nathan, A. C. Ferrari, W. I. Milne, *J. Appl. Phys.* **2007**, *102*, 043710.
[27] H. Okimoto, T. Takenobu, K. Yanagi, Y. Miyata, H. Shimotani, H. Kataura, Y. Iwasa, *Adv. Mater.* **2010**, *22*, 3981.
[28] X. Liang, J. Xia, G. Dong, B. Tian, L. Peng, *Top. Curr. Chem.* **2016**, *374*, 80.
[29] S. Park, M. Vosguerichian, Z. Bao, *Nanoscale* **2013**, *5*, 1727.
[30] J. P. V. Damasceno, A. J. G. Zarbin, *Chem. Commun.* **2019**, *55*, 5809.
[31] K. D. Ausman, R. Piner, O. Lourie, R. S. Ruoff, M. Korobov, *J. Phys. Chem. B* **2000**, *104*, 8911.
[32] D. Kiriya, K. Chen, H. Ota, Y. Lin, P. Zhao, Z. Yu, T. J. Ha, A. Javey. *J. Am. Chem. Soc.* **2014**, *136*, 11188.
[33] P. Chen, Y. Fu, R. Aminirad, C. Wang, J. Zhang, K. Wang, K. Galatsis, C. Zhou, *Nano Lett.* **2011**, *11*, 5301.
[34] H. Wang, Y. Wang, H. Yan, J. Zhang, R. K. Thomas, *Langmuir* **2006**, *22*, 1526.
[35] M. A. Winnik, S. M. Bystryak, C. Chassenieux, V. Strashko, P. M. Macdonald, J. Siddiqui, *Langmuir* **2000**, *16*, 4495.

 © 2020 WILEY-VCH Verlag GmbH & Co. KGaA, Weinheim

[36] J. E. Rossi, K. J. Soule, E. Cleveland, S. W. Schmucker, C. D. Cress, N. D. Cox, A. Merrill, B. J. Landi, *J. Colloid Interface Sci.* **2017**, *495*, 140.
[37] Z. Sun, V. Nicolosi, D. Rickard, S. D. Bergin, S. D. Aherne, J. N. Coleman, *J. Phys. Chem. C* **2008**, *112*, 10692.
[38] J. P. Opatkiewicz, M. C. LeMieux, Z. Bao, *ACS Nano* **2010**, *4*, 1167.
[39] J. Tittmann-Otto, S. Hermann, J. Kalbacova, M. Hartmann, M. Toader, R. D. Rodriguez, S. E. Schulz, D. R. T. Zahn, T. Gessner, *J. Appl. Phys.* **2016**, *119*, 124509.
[40] V. K. Sangwan, A. Behnam, V. W. Ballarotto, M. S. Fuhrer, A. Ural, E. D. Williams, *Appl. Phys. Lett.* **2010**, *97*, 043111.
[41] C. Kocabas, N. Pimparkar, O. Yesilyurt, S. J. Kang, M. A. Alam, J. A. Rogers, *Nano Lett.* **2007**, *7*, 1195.
[42] V. K. Sangwan, R. P. Ortiz, J. M. P. Alaboson, J. D. Emery, M. J. Bedzyk, L. J. Lauhon, T. J. Marks, M. C. Hersam, *ACS Nano* **2012**, *6*, 7480.
[43] N. Rouhi, D. Jain, K. Zand, P. J. Burke, *Adv. Mater.* **2011**, *23*, 94.
[44] J. Zhang, Y. Fu, C. Wang, P. C. Chen, Z. Liu, W. Wei, C. Wu, M. E. Thompson, C. Zhou, *Nano Lett.* **2011**, *11*, 4852.
[45] M. Shimizu, S. Fujii, T. Tanaka, H. Kataura, *J. Phys. Chem. C* **2013**, *117*, 11744.
[46] E. X. Ding, Q. Zhang, N. Wei, A. T. Khan, E. I. Kauppinen, *R. Soc. Open Sci.* **2018**, *5*, 180392.
[47] C. W. Lee, C. H. Weng, L. Wei, Y. Chen, M. B. Chan-Park, C. H. Tsai, K. C. Leou, C. H. P. Poa, J. Wang, L. J. Li, *J. Phys. Chem. C* **2008**, *112*, 12089.
[48] M. Y. Timmermans, D. Estrada, A. G. Nasibulin, J. D. Wood, A. Behnam, D. M. Sun, Y. Ohno, J. W. Lyding, A. Hassanien, E. Pop, E. I. Kauppinen, *Nano Res.* **2012**, *5*, 307.
[49] S. P. Schießl, X. De Vries, M. Rother, A. Massé, M. Brohmann, P. A. Bobbert, J. Zaumseil, *Phys. Rev. Mater.* **2017**, *1*, 046003.
[50] J. Liang, L. Li, D. Chen, T. Hajagos, Z. Ren, S. Y. Chou, W. Hu, Q. Pei, *Nat. Commun.* **2015**, *6*, 7647.

© 2020 WILEY-VCH Verlag GmbH & Co. KGaA, Weinheim